BIAS VOLTAGE CONTROL OF A MOLECULAR SPIN VALVE

A THESIS

SUBMITTED TO THE DEPARTMENT OF PHYSICS

AND THE INSTITUTE OF ENGINEERING AND SCIENCE

OF BILKENT UNIVERSITY

IN PARTIAL FULFILLMENT OF THE REQUIREMENTS

FOR THE DEGREE OF

MASTER OF SCIENCE

By

Duygu Can

August 2009

I certify that I have read this thesis and that in my opinion it is fully adequate, in scope and in quality, as a dissertation for the degree of master of science.

Prof. Salim Çıracı (Supervisor)

I certify that I have read this thesis and that in my opinion it is fully adequate, in scope and in quality, as a dissertation for the degree of master of science.

Assoc. Prof. Ramazan Tuğrul Senger

I certify that I have read this thesis and that in my opinion it is fully adequate, in scope and in quality, as a dissertation for the degree of master of science.

Assist. Prof. Hande Toffoli (Üstünel)

I certify that I have read this thesis and that in my opinion it is fully adequate, in scope and in quality, as a dissertation for the degree of master of science.

Assoc. Prof. Mehmet Özgür Oktel

I certify that I have read this thesis and that in my opinion it is fully adequate, in scope and in quality, as a dissertation for the degree of master of science.

Assist. Prof. Coşkun Kocabaş

Approved for the Institute of Engineering and Science:

Prof. Mehmet Baray,
Director of Institute of Engineering and Science

Abstract

BIAS VOLTAGE CONTROL OF A MOLECULAR SPIN VALVE

Duygu Can
MSc in Physics
Supervisor: Prof. Salim Çıracı
Cosupervisor: Assoc. Prof. Ramazan Tuğrul Senger
August 2009

With the discovery of giant magneto resistance a new field called spintronics is emerged. Utilizing spin-degree of freedom of the electron as well as its charge, high-speed devices which consumes low energy can be designed. One of the main concerns of spintronics is creating spin polarized currents. Half-metallic materials, which conduct electrons of one spin state but behave as an insulator for the other spin state, are ideal candidates for this purpose. In a way they function as spin-valves, and the current passing through these materials will be spin polarized. The half-metallic property of periodic atomic chains of carbon-transition metal compounds and spin-valve property of transition metal caped finite carbon linear chains motivated our study. In this work, we analyzed the spin dependent transport properties of CrC_nCr atomic chains. We connected the magnetic CrC_nCr molecules to appropriate electrodes and studied their electronic and magnetic properties under applied bias. All the calculations are carried out using a method which combines density functional theory (DFT) with non-equilibrium Green's function (NEGF) technique. For CrC_nCr molecules with odd n we

observed cumulenic bond lengths, while the $C-C$ bonds are in polyynic nature for even n. In these structures Cr atoms induce net magnetic moments on C atoms. The magnetic moment on Cr atoms favors anti-parallel (AF) alignment for even n and parallel (FM) alignment for odd n. This situation is inverted when the molecules are connected to the electrodes. Two-probe conductance calculations of such systems reveal that their conductance properties are also n dependent. Finite bias voltages which create non-equilibrium conditions within the device region, causes the spin-degenerate molecular levels of the device to be separated from each other. Then conductance properties of the device become spin dependent. We observe that the ground state CrC_nCr two-probe systems with odd n changes from AF to FM at a critical voltage. Thus, we have a spin-valve which is initially in "off-state" turned on with applied bias. We achieved to control spin-polarization of the current transmitted through a molecular spin-valve with applied bias voltage. We showed that they are molecular analogues of GMR devices. These molecular spin-valve devices function without any need of an external magnetic field as it is required in conventional GMR devices.

Keywords: molecular electronics, spintronics, quantum transport, carbon linear chain, transition metal atom, ballistic conductance.

Özet

BİR MOLEKÜLER SPİN SÜZGECİNİN ÖNGERİLİM VOLTAJI İLE KONTROLÜ

Duygu Can
Fizik Yüksek Lisans
Tez Yöneticisi: Prof. Dr. Salim Çıracı
İkinci Tez Danışmanı: Doç. Dr. Ramazan Tuğrul Senger
Ağustos 2009

Dev manyetik direncin (DMD) keşfedilişi ile spintronik adında yeni bir alan ortaya çıktı. Yükünün yanı sıra, elektronun spin serbestlik derecesini de kullanılması daha az enerji tüketen yüksek hızlı aygıtlar tasarlanmasına fırsat verir. Spintroniğin ana hedeflerinden biri spin kutuplu akım yaratabilmektir. Bir spin durumlu elektronlara ileten ama diger spin durumlu elektronlar icin yalıtkan gibi davranan yarım-metalik malzemeler bu amaç için uygun adaylardır. Bir bakıma spin süzgeci gibi çalışırak ve geçen akım spin kutuplu yaparlar. Karbon-geçiş metali bileşiklerinin periyodik yapılarının yarım-metal özelliği ve geçiş metali kaplı doğrusal karbon zincirlerinin spin süzgeci özelliği bizi bu çalışmaya sevketmiştir.

Bu çalışmada, CrC_nCr atomik zincirlerinin spin bağımlı iletkenlik özellikleri incelenmiştir. Uygun elektrotlara bağlanmış CrC_nCr manyetik moleküllerinin gerilim altındaki elektronik ve manyetik özellikleri çalışılmıştır. Tüm hesaplamalar durum yoğunluğu teorisini, denge dışı Green fonksiyonu tekniğini birleştiren bir metodla yapılmıştır.

Tek n sayılı CrC_nCr moleküllerde $C-C$ bağları kümülenik karakterdeyken, çift sayılı yapılarda poli-alkin karakterdedir. Bu yapılarda Cr atomları C atomları üzerinde net manyetik momentler indüklerler. Çift n sayılı yapılarda Cr atomları üzerindeki net manyetik momentler birbirlerine ters(AF) olacak şekilde hizalanmayı secerken, tek n sayılı yapılarda birbirlerine paralel(FM) olurlar. Bu durum molekül elektrodlara bağlanınca tersine döner. Böyle sistemlerin iki uçlu iletkenlik hesapları gösterir ki iletkenlik özellikleri de n'ye bağlıdır. Aygıt bölgesinde denge dışı durum yaratan gerilim voltajı, spin-dejenere moleküler seviyelerin birbirinden ayrılmasına neden olur. Bu durumda iletkenlik özellikleri spine bağlı olarak değişir. Tek sayılı CrC_nCr iki uçlu siteminin temal durumu belirli bir voltajda AF'den FM'ye değiştiği gözlemlenmektedir. Böylelikle başlangıçta kapalı durumda olan spin süzgeci gerilim altında açılmış olur.

Moleküler bir spin süzgecinden gecen spin kutuplu akımın gerilim voltajı ile kontrolü gösterilmiştir. Bu yapılar DMD aygıtlarının moleküler boyutta bir benzeridirler. Bu tür moleküler spin süzgeçleri geleneksel DMD aygıtlarının çalışması için gereken manyetik alanlar olmaksızın da işlev gösterebilirler.

Anahtar sözcükler: molekül elektroniği, spintronik, kuvantum taşınım, doğrusal karbon zinciri, geçiş metali atomu, balistik iletkenlik.

Acknowledgement

First of all I would like to express my sincere appreciation to my thesis advisors Prof. Salim Çıraçı and R. Tuğrul Senger for their valuable guidance.

I am grateful to my friends at Bilkent with whom I enjoyed much.

I offer my sincere thankfulness to my family for their support.

I am grateful to the my cast crew: İlker Ocaklı, Selma Şenozan, Levent Şubaşı, Özgür Bayındır, Kerem Altun, Cem Murat Turgut, Ümit Keleş, Selcen Aytekin, Can Rıza Afacan and Cemal Albayrak. I could not even finish this thesis without their encouragement and support.

I am also thankful to BİDEP 2228 scholarship provided by TÜBİTAK which supported my graduate studies.

Contents

List of Figures

List of Tables

Chapter 1

Introduction

The well known effect giant magneto resistance (GMR) can be observed in layered structures [1, 2]. In the GMR effect change in the relative alignment of the magnetization of the layers dramatically affects the resistance of the material. A GMR spin-valve shown in Fig.1.1 is a device which is composed of two magnetic layers separated by a non-magnetic metal. A coating of an antiferromagnetic layer is also grown over the uppermost ferromagnetic layer to pin the magnetization of the layer below through exchange bias. Since antiferromagnets has no net magnetic moments, their spin orientation is weakly influenced by an external magnetic field. The inter-facial spins of the ferromagnet that is strongly coupled to the antiferromagnet will be pinned. This is the basic mechanism under the phenomena of magnetization pinning. The magnetization of the other magnetic layer at the bottom is free to rotate. The direction of the magnetization of the free layer can be tuned by applied magnetic field. When the magnetization of the ferromagnetic layers are parallel, the electrons with the same spin alignment are transmitted without being subject to any spin dependent scattering from the interface between ferromagnetic and non-magnetic layers, whereas the electrons with the opposite spin alignment are scattered from both interfaces. When the magnetization of the ferromagnetic layers are anti-parallel, electrons of both spin states are scattered. Thus resistance is higher for anti-parallel alignment than the parallel case. The magnetoresistance is the change in the resistance

of the material with the applied external magnetic field. The difference in the conduction between the parallel and the antiparallel magnetization of the ferromagnetic layers is high for such layered structures.

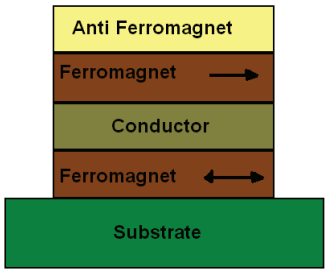

Figure 1.1: Schematic view of a GMR device

In a very short time after the invention, the mass produced technology of GMR effect is used in mass produced devices such as the read head of the standard hard drives [3]. The discovery of GMR not only brought Nobel prize to Fert and Grüunberg in 2007, but also initiated a new field called spintronics. Spintronics is a made-up word meaning spin-electronics. The spintronics benefits from utilizing spin degree of freedom of the electron as well as its charge and this results in a higher information capacity than the conventional electronic devices. The energy scale for manipulating the spin is order of times smaller than changing the charge in conventional electronics [3]. The spintronic devices are expected to be more efficient because of their properties of non-volatility, high speed, low energy consumption and high integration densities [4].

Now this new-born field of spintronics is expanding through 'molecular spintronics'. One of the main applications of this new axis is the molecular spin-valve. The electrical resistance of the spin-valve changes depending on the relative alignment of the magnetization of the electrodes and the molecule in between [5]. The first examples of molecular spin-valves composed of a buckyball and a carbon nanotube with magnetic contacts are already realized [6, 7].

Half-metallic materials are perfect candidates for spin-valve applications due

to their intrinsic spin imbalance in the charge carriers. The concept of half-metallicity introduced by De Groot et al. [8] arises from the distinct feature of spin-dependent band structure of such materials. As it is visualized in Fig.1.2 only one of the spin bands crosses the Fermi level, whereas for the other band the Fermi level lies in the band-gap. Thus, half-metals conduct electrons of one spin state but behave as an insulator for the other spin state. In a way they function as spin-valves, and the current passing through these materials will be spin-polarized. It is found that periodic atomic chains of carbon-transition metal

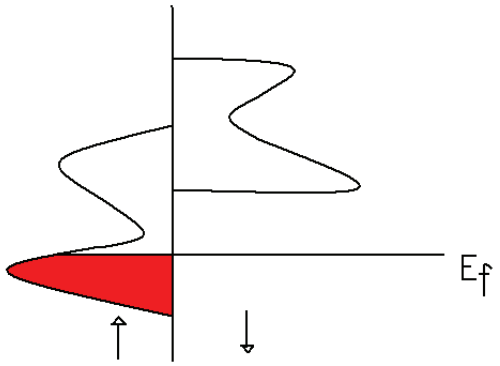

Figure 1.2: Schematic view of band structure of a half-metallic structure

(C_nTM) compounds are half-metallic [9]. It is also reported that transition metal caped finite carbon linear chains ($TM{-}C_n{-}TM$) show strong spin-valve effect when connected to the electrodes and are molecular analogue of conventional GMR devices [10, 11]. These studies are inspiring for our research of using chromium caped atomic strings of carbon (CrC_nCr) to create spin polarized currents. The structural, electronic, magnetic and transport properties of these materials are systematically analyzed.

The main purpose of this study is to control spin-polarization of the current with bias voltage. Finite bias voltages which create non-equilibrium conditions within the device region, causes the spin-degenerate molecular levels of the device

to be separated from each other. Since the conductance is related to number of states available around the Fermi level, different contributions come from these split states and the conductance properties of the device become spin dependent. With this new approach the spin-valve functions as the electric current passes through it without any need of an external magnetic field.

The organization of the thesis is as follows: a brief discussion of the theory is given in Chapter 2. The transition metal caped carbon linear chains are studied in Chapter 3. The two-probe conductance calculations of the structures discussed in the previous chapter are given in Chapter 4. In Chapter 5 as a conclusion part, the obtained results are briefly summarized.

Chapter 2

Methodology

2.1 The Many-Body Hamiltonian

To understand the physical and chemical properties of the systems which are more complex than the Hydrogen atom, one should deal with the many-body Hamiltonian. The Hamiltonian of interacting particles, say an ionic crystal, can be written in atomic units as follows:

$$\begin{aligned} H &= -\frac{\hbar^2}{2m}\sum_{i=1}^{n}\nabla_i^2 + \frac{1}{2}\sum_{i=1}^{n}\sum_{j\neq i}^{n}\frac{1}{|\mathbf{r}_i-\mathbf{r}_j|} - \sum_{I=1}^{N}\sum_{i=1}^{n}\frac{Z_I}{|\mathbf{R}_I-\mathbf{r}_i|} \\ &\quad -\frac{\hbar^2}{2M_I}\sum_{I=1}^{N}\nabla_I^2 + \sum_{I=1}^{N}\sum_{J\neq I}^{N}\frac{Z_I Z_J}{|\mathbf{R}_I-\mathbf{R}_J|} \end{aligned} \tag{2.1}$$

where $\mathbf{r}$ =$(\mathbf{r}_i, i = 1, ..., n)$ is a set of n electron coordinates $\mathbf{R}$ =$(\mathbf{R}_I, I = 1, ..., N)$ is a set of N ionic coordinates. Z_I are ionic charges and M_I are ionic masses. The factor of $\frac{1}{2}$ has been included in order to avoid double counting of terms. The terms in Eqn.2.1 are kinetic energy of the electrons, electron-electron interaction, electron-ion interaction, the kinetic energy of the ions and ion-ion interaction respectively. Inserting this Hamiltonian into the Schrödinger equation and solving for the eigenfunction is almost impossible except for a few trivial cases. Not to deal with $3n + 3N$ degrees of freedom, some approximation methods should be

employed.

2.2 Approximations to Simplify the Many-Body Problem

2.2.1 Born-Oppenheimer Approximation

The first approximation to simplfy the problem is the Born-Oppenheimer approximation [12]. Since the mass of the electrons are much smaller than the ions, electrons move much faster. Thus the electrons immediately give response to any change in the ionic positions. The ions are assumed to be stationary. Their ionic kinetic energy term in Eqn.2.1 can be neglected. This approximation is not enough to simplify the many-body Hamiltonian alone. The problem remains unsolvable except for a few cases such as free electron gas.

2.2.2 Hartree and Hartree-Fock Approximations

According to Hartree [13] the many-electron wave function can be approximated by a product of one-electron wave-functions as

$$\Phi(\mathbf{R},\mathbf{r}) = \phi_1(\mathbf{r}_1)\phi_2(\mathbf{r}_2),\ldots,\phi_N(\mathbf{r}_N) \tag{2.2}$$

and each of these one-electron wave functions satisfies one-particle Schrödinger equation

$$\left(-\frac{\hbar^2}{2m}\nabla^2 + V_{eff}^{(i)}(\mathbf{R},\mathbf{r})\right)\phi_i(\mathbf{r}) = \varepsilon_i\phi_i(\mathbf{r}) \tag{2.3}$$

where the second term in parenthesis is the effective potential. Through this effective potential each electron feels the presence of the other electrons.

$$V_{eff}^{(i)}(\mathbf{R},\mathbf{r}) = V_{ext}(\mathbf{R},\mathbf{r}) + \int \frac{\sum_{j\neq i}^{N}\rho_j(\mathbf{r}')}{|\mathbf{r}-\mathbf{r}'|}d\mathbf{r}' \tag{2.4}$$

with charge density of the paticle j defined as

$$\rho_j(\mathbf{r}) = |\phi_j(\mathbf{r})|^2 \tag{2.5}$$

where the last term is called the Hartree potential. The energy is given by

$$E^H = \sum_i^N \varepsilon_i - \frac{1}{2}\int\int \frac{\rho_j(\mathbf{r})\rho_j(\mathbf{r}')}{|\mathbf{r}-\mathbf{r}'|} d\mathbf{r}d\mathbf{r}' \tag{2.6}$$

where the 1/2 term added not to count the same electron-electron interaction twice. Using variational methods energy is minimized with respect to a set of parameters in a trial wave function. The charge density that is calculated from the minimized wave function is later used in determining the effective potential. Then the one-particle Schrödinger equation solved again. This procedure is repeated until the self-consistency is reached.

The Hartree approximation is further improved via inclusion of the Pauli exclusion principle. Since the particles in question are electrons the total wave function must be anti-symmetric and can be formulated as a Slater detarminant.

$$\Phi = \frac{1}{\sqrt{N!}} \begin{pmatrix} \phi_1(\mathbf{x}_1) & \dots & \phi_1(\mathbf{x}_N) \\ \vdots & \ddots & \vdots \\ \phi_N(\mathbf{x}_1) & \dots & \phi_N(\mathbf{x}_N) \end{pmatrix}$$

This is called Hartree-Fock approximation and it is a wavefunction based approximation[14, 15].

2.2.3 Thomas-Fermi Approximation

In this method the kinetic energy is represented as a functional of electron density[16, 17]. The approximation lacks in representation of exchange energy. Later local approximation for exchange was added by Dirac[18]. It is the ancestor of Density Functional Theory (DFT).

2.3 Density Functional Theory

Density functional theory (DFT) is a very powerful tool for calculating the electronic structure using functionals of the electron density [19, 20]. The ground state electron density uniquely determines the system. DFT includes exchange and correlation energies. Differing from its ancestors DFT is an exact theory.

2.3.1 The Hohenberg-Khon Theorem and the Khon-Sham Equations

Two theorems lies beneath DFT as Hohenberg and Kohn formulated[19]:

Theorem 1**:** The external potential is a unique functional of the electron density.

Theorem 2**:** A universal functional for the energy $E[n]$ can be defined in terms of the electron density. The exact ground state is the global minimum value of this functional.

The Hohenberg-Kohn theorems are used to obtain the orbitals that give rise to ground state energy, the total energy is minimized with respect to the orbitals [20, 21].

$$E = min \frac{\left\langle \tilde{\Psi} | H | \tilde{\Psi} \right\rangle}{\left\langle \tilde{\Psi} \tilde{\Psi} \right\rangle} \tag{2.7}$$

Charge density, $\tilde{\rho}$, can be used instead of $\tilde{\Psi}$. When the $\tilde{\rho}$ is the ground state density, the minimum in energy is obtained. The energy can be presented as

$$E_V[\tilde{\rho}] = F[\tilde{\rho}] + \int \tilde{\rho}(\mathbf{r}) V(\mathbf{r}) d\mathbf{r} \tag{2.8}$$

with the universal functional

$$F[\tilde{\rho}] = \left\langle \Psi[\tilde{\rho}] | \hat{T} + \hat{U} | \Psi[\tilde{\rho}] \right\rangle \tag{2.9}$$

where $\Psi[\tilde{\rho}]$ is the ground state of a potential $\hat{U}$ which has $\tilde{\rho}$ as charge density and $V(\mathbf{r})$ is the external potential.

When non-interacting electrons in a system create the same electronic density of the interacting system, the kinetic energy of the non-interacting system can be calculated[20]. Which means that, the kinetic energy of the interacting electrons is replaced by that of the non-interacting system. In this assumption the charge density is

$$\rho(\mathbf{r}) = \sum_{i=1}^{N} |\varphi_i(\mathbf{r})|^2 \tag{2.10}$$

and the kinetic energy is

$$T[\rho] = -\sum_{i=1}^{N} \left\langle \varphi_i | \frac{\nabla^2}{2} | \varphi_i \right\rangle \tag{2.11}$$

Here the φ_i are single particle orbitals. The universal functional takes the form

$$F[\tilde{\rho}] = T[\rho] + \frac{1}{2} \int \int \frac{\rho(\mathbf{r})\rho(\mathbf{r}')}{|\mathbf{r} - \mathbf{r}'|} d\mathbf{r} d\mathbf{r}' \tag{2.12}$$

where in the last term exchange and correlation energy is defined as a functional of the density. Inserting the equation above into Eqn.2.8 we obtain the total energy functional

$$E_{KS}[\rho] = T[\rho] + \int \rho(\mathbf{r}) \upsilon(\mathbf{r}) d\mathbf{r} + \frac{1}{2} \int \int \frac{\rho(\mathbf{r})\rho(\mathbf{r}')}{|\mathbf{r} - \mathbf{r}'|} d\mathbf{r} d\mathbf{r}' + E_{XC}[n] \tag{2.13}$$

The density functional represented in terms of the Kohn-Sham orbitals which minimize the kinetic energy under the constraint of fixed density. The solution of Kohn-Sham equations has to be obtained self consistently.

2.4 Exchange-Correlation Functionals

Although DFT is an exact theory, the exchange and the correlation energies are not known explicitly. Thus their sum is approximated.

2.4.1 The Local Spin Density Approximation (LSDA)

In the limit of the homogeneous electron gas the effects of exchange and correlation is local and local spin density approximation (LSDA) is valid [22]. In this approximation the inhomogenous electronic system is treated as locally homogenous. The exchange-correlation energy is an integral over all space with the exchange-correlation energy density at each point assumed to be the same as in a homogeneous electron gas with that density,

$$E_{xc}^{LSDA}[\rho^{\uparrow}, \rho^{\downarrow}] = \int d^3 r \rho(\mathbf{r}) \epsilon_{xc}^{hom}(\rho^{\uparrow}(\mathbf{r}), \rho^{\downarrow}(\mathbf{r})) \tag{2.14}$$

Figure 2.1: Schematic view of a conductor (C) connected to left (L) and right (R) leads

where ϵ_{xc}^{hom} is the exchange correlation energy density. When we set $\rho^{\uparrow}(\mathbf{r}) = \rho^{\downarrow}(\mathbf{r}) = \rho(\vec{\mathbf{r}})/2$ we obtain the same approximation for spin-unpolarized systems (LDA).

The LSDA works better for the systems close to a homogeneous gas.

2.4.2 Generalized Gradient Approximation (GGA)

Expanding the density in terms of the gradient and the higher other derivatives, LSDA is further improved[23]. The new approximation is the generalized gradient approximation (GGA) and the basic form of exchange-correlation energy can be written as;

$$E_{xc}^{GGA}[\rho^{\uparrow}, \rho^{\downarrow}] = \int d^3r \rho(\mathbf{r}) \epsilon_{xc}^{hom}(\rho) F_{xc}(\rho^{\uparrow}, \rho^{\downarrow}, \nabla\rho^{\uparrow}, \nabla\rho^{\downarrow}, ...) \qquad (2.15)$$

where ϵ_{xc}^{hom} is the exchange correlation energy and F_{xc} is a dimensionless factor that upgrades the LDA expression according to the variation of the density. Different forms of F_{xc} have been proposed by Becke(B88)[24], Perdew and Wang(PW91)[25] and Perdew, Burke and Enzerhof(PBE)[23].

2.5 Electronic Transport

Through the Landauer formula, the conductance of a device connected to leads (Fig.2.1) is related to its scattering probability[26]:

$$G = \frac{2e^2}{h}T \tag{2.16}$$

where T is the transmission function and G is the conductance. Later we will write this transmission function in terms of Green's functions.

2.5.1 Equilibrium Case

In Green's function formalism whenever response R is related to the excitation S by a differential operator D_{op}

$$D_{op}R = S \tag{2.17}$$

we can define the Green's function as

$$R = GS \tag{2.18}$$

thus

$$G = D_{op}^{-1} \tag{2.19}$$

In transport phenomena we deal with Schrödinger equation with an incident wave from the leads, S.

$$[E - H]\Psi = S \tag{2.20}$$

So the Green's function of the system is

$$G = [E - H]^{-1} \tag{2.21}$$

The equation above has two solutions for outgoing and incoming waves which are the retarded and the advanced Green's functions respectively.

$$\begin{aligned} G^R &= [E + i\eta - H]^{-1} \\ G^A &= [E - i\eta - H]^{-1} = [G^R]^\dagger \end{aligned} \tag{2.22}$$

where η is a small number to separate two solutions. The retarded and advanced Green's functions Hermitian conjugates.

Expanding the Hamiltonian operator of the system in a local basis we obtain the matrix form

$$H = \begin{pmatrix} [H_L]_{\infty\times\infty} & [h_{LC}]_{\infty\times n} & 0 \\ [h_{CL}]_{n\times\infty} & [H_C]_{n\times n} & [h_{CR}]_{n\times\infty} \\ 0 & [h_{RC}]_{\infty\times n} & [H_R]_{\infty\times\infty} \end{pmatrix} \tag{2.23}$$

where H_C, H_L and H_R are Hamiltonians of the conductor and the semi-infinite left and right leads respectively. h_{CR} and h_{CL} are the coupling matrices of the conductor to the electrodes. Since we use a local basis there is no interaction with left and right electrodes, the corresponding part is null in the Hamiltonian. When we insert 2.23 into 2.21 we can obtain the Green's function in matrix form which can be further partitioned into submatrices of the individual subsystems $(L - C - R)$.

$$\begin{pmatrix} G_L & G_{LC} & G_{LCR} \\ G_{CL} & G_C & G_{CR} \\ G_{LRC} & G_{RC} & G_R \end{pmatrix} = \begin{pmatrix} \epsilon - H_L & h_{LC} & 0 \\ h_{LC}^\dagger & \epsilon - H_C & h_{CR} \\ 0 & h_{CR}^\dagger & \epsilon - H_R \end{pmatrix}^{-1} \tag{2.24}$$

where $\epsilon - H_C$ represents finite isolated conductor and $\epsilon - H_{R,L}$ represent infinite leads. G_C represents all the dynamics about the electrons inside the conductor including the effect of the electrodes. G_C can be formulated as[27]

$$G_C = (\epsilon - H_C - \Sigma_L - \Sigma_R)^{-1} \tag{2.25}$$

where $\Sigma_L = h_{LC}^\dagger g_L h_{LC}$ and $\Sigma_R = h_{RC}^\dagger g_R h_{RC}$ are the self-energy terms due to semi-infinite leads and $g_{L,R} = (\epsilon - H_{L,R})^{-1}$ are the Green's functions of the leads. When a molecule connected to the leads, its all molecular levels shift in energy and this infinitely sharp levels get broaden due to coupling with the leads. The imaginary part of the self-energy term represents the broadening of the levels and the real part represents the shift in the energy. Thus, overall effect of the infinite leads on the conductor is represented exactly by these self-energy terms. The

broadening matrices which describe the strength of the coupling of leads to the conductor can be calculated from these self-energy matrices[27].

$$\Gamma_{L,R} = i[\Sigma^r_{L,R} - \Sigma^a_{L,R}] \qquad \text{with} \qquad \Sigma^r_{L,R} = {\Sigma^a_{L,R}}^\dagger \tag{2.26}$$

where $\Sigma^r_{L,R}$ and $\Sigma^r_{L,R}$ are the retarded and the advanced self-energy terms. Once the Green's functions and broadening matrices are known, the transmission function can be calculated

$$T = \mathrm{Tr}(\Gamma_L G^r_C \Gamma_R G^a_C) \tag{2.27}$$

Substituting Eqn.2.27 into Eqn.2.16, we can calculate the conductance.

The nature of the allowed electronic states can be described by the spectral function

$$A = i(G^r_C - G^a_C) \tag{2.28}$$

of which diagonal elements give the density of states

$$D(E) = \frac{1}{2\pi}\mathrm{Tr}[A(E)] \tag{2.29}$$

By integrating the spectral function over filled states we obtaion the density matrix

$$[\rho] = \frac{1}{2\pi}\int dE f(E,\mu)A(E) \tag{2.30}$$

In DFT based Green's function method charge density is obtained by diagonalizing the density matrix. Since the external potential is a unique functional of charge density in DFT, we can also obtain Hamiltonian of the system. From the Hamiltonian, the Green's function of the conductor can be calculated as described above. Finally this Green's function is used again to calculate the charge density. This procedure is continued until the self-consistency is reached. So that the transport properties of the conductor is calculated in equilibrium conditions.

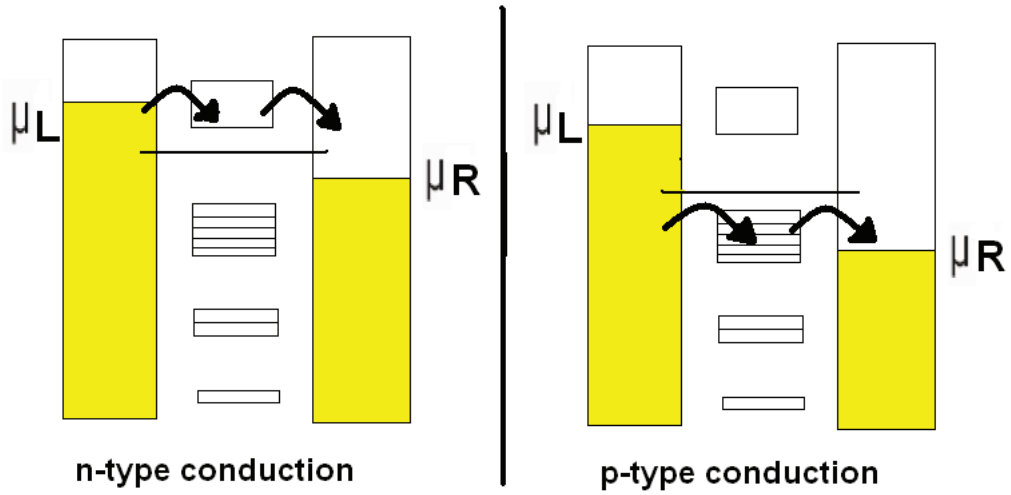

Figure 2.2: Energy level diagram of a device connected electrodes. n-type (left) and p-type (right) conduction is illustrated

2.5.2 Non-equilibrium Case

In the non-equilibrium case the leads no longer share the same chemical potential. Their Fermi functions are different.

$$\begin{aligned} f_L &= \frac{1}{1+\exp[(\epsilon-\mu_L)/k_BT]} \\ f_R &= \frac{1}{1+\exp[(\epsilon-\mu_R)/k_BT]} \end{aligned} \tag{2.31}$$

So the density matrix changes to

$$[\rho] = \frac{1}{2\pi}\int dE(f(E,\mu_L)A_L(E) + f(E,\mu_R)A_R(E)) \tag{2.32}$$

where $A_L = G^r\Gamma_L G^a$ and $A_R = G^r\Gamma_L G^a$ are left and right components of the spectral function. The self-consistent cycle is the same with the equilibrium case.

Each contact tries to bring the channel in equilibrium with itself. Due to their different agenda this competition never ends and the current flows[27].

$$I = \frac{2e}{h}\int dE(f_L - f_R)T(E) \tag{2.33}$$

where T(E) is the transmission function and given in Eqn.2.27. In this way the current is calculated self-consistently at finite bias voltages.

The concept of quantum transport can also be understood from Fig.2.2. The conductance depends availability of the states around average potential of the electrodes, μ. When the transport occurs through empty states, it is called n-type otherwise it is called p-type. Only the states lies within $\mu_1 - \mu_2$ contributes to the conduction. Coupling of the electrodes to the channel inevitably broadens the energy levels which results in spreading of the level outside energy range between μ_1 and μ_2. The levels also align themselves with contact potentials, this results in shift in the energy. Example of such properties will be discussed in Chapter 4.

Chapter 3

Atomic Chains of Carbon

Monatomic linear chains of carbon have been studied for decades and their interesting electronic transport properties have been revealed[9–11, 28–31]. Ab-initio studies suggest that free standing infinite chains of carbon are metallic [32]. For this reason they can be used as building blocks in electronics applications at the nano-scale. Carbon linear chains(CLCs) were experimentally realized, so this is not just an academic problem anymore. For example, CLCs were already prepared in solution [33] using chemical methods. It is also predicted by a density functional study [34] and later observed by using arc discharge technique [35, 36] that carbon linear chains form stable structures inside multi-walled carbon nanotubes. However, to make them function as a component of a molecular device, they must be synthesized in a more effective way. Recently, a more controlled and reliable method to synthesize CLCs has been developed. By continuously thinning a graphene nanoribbon from its ends, free standing carbon atomic rows of one or two atom thickness can now be fabricated [37]. Thus, the dream of using conducting CLCs as a component in molecular electronics could be turned into reality.

3.1 Transition Metal Caped Carbon Linear Chains

One way to obtain spin-dependent electronic transport properties is functionalizing CLCs with magnetic atoms. Dag et al. studied carbon-transition metal compounds(C_nTM) by DFT calculations and found that they exhibit half-metallic properties [9]. In their study a large family of C_nTM chains is covered choosing transition metal atoms as chromium, titanium, manganese and iron. The spin-dependent electron band structures of C_nTM periodic structures strongly depend on the number of carbon atoms, n, in the supercell. This dependence is explained by the difference in bonding patterns of C_nTM chains. For odd n cumulene ($TM{=}C{\cdots}C{=}C{=}C{\cdots}C{=}TM$), for even n polyyne ($TM{-}C{\cdots}C{\equiv}C{-}C{\equiv}C{\cdots}C{-}TM$) bonds are formed. Whether the bond between TM and C is single or double changes the length of the bonds and as a result the overlap between TM and C orbitals is changed. Thus the relative energy positions of bands vary.

(a) AF (b) FM

Figure 3.1: (a)Anti-ferromagnetic and (b)ferromagnatic states of an isolated $TM{-}C_n{-}TM$ chain. TM atoms are donated by large(blue) spheres and small(grey) spheres are for C atoms.

In other studies carried out by the same group, it is shown that finite segments

of CLCs caped with transition metal atoms($TM-C_n-TM$) show strong spin-valve effect when connected to the metallic electrodes [10, 11, 31]. The magnetic ground state of these isolated chains alternate between ferromagnetic(FM) and anti-ferromagnetic(AF) states as a function of the number of carbon atoms in between transition metals, n as shown in Fig.3.1. They claim that the type of the TM atom determines whether odd or even n leads to AF ground state. Similar to [9], in even n cases the structures are dimerized, while $C-C$ bonds remain almost constant for odd n. It is found that C atoms acquire alternating magnetic moments due to coupling with the magnetic TM atom. This induced magnetic moments on C atoms invokes indirect exchange interaction between the TM atoms. Furthermore, the $TM-C_n-TM$ chain connected to the gold electrodes and its conductance properties are investigated. The conductance properties also depends on the coupling of the device with the electrodes. Contrasting to AF state, the conductance of the FM state is spin-polarized and attains higher values.

The half-metallicity observed in the spin-dependent band structures of C_nTM compounds [9] and spin-valve property of $TM-C_n-TM$ magnetic molecules [10, 11, 31] motivated our research. These works are also a part of the thesis submitted by E. Durgun [31] for the degree of doctor of philosophy in physics to the Institute of Engineering and Science at Bilkent University. In the light of these previous studies, we repeated the calculations for CrC_nCr molecular structures with $n = 0, 1, 2, 3, 4, 5$ since they are appropriate for spintronics applications.

We have performed first-principles total energy calculations to reproduce electronic structure and optimized geometry of CrC_nCr molecules within density functional theory [19, 20] using the software package Atomistix ToolKit(ATK) [38]. The spin-dependent exchange-correlation potential is approximated within the generalized gradient approximation(GGA) [23]. During the optimization calculations Bloch wave functions have been expanded by double-zeta-polarized basis sets of local numerical orbitals whose kinetic energies are smaller than 150 Ryd. Atomic positions are optimized using steepest descent method. The convergence is achieved when the change in the total energy of the system between two successive ionic steps falls below 10^{-4} Ryd. and the Hellman-Feynman forces

on the atoms falls below a tolerance of 0.05 eV/Å.

In agreement with the previous works [10, 11, 31], relative alignment of the magnetization of Cr atoms is parallel(FM) for odd n and anti-parallel(AF) for even n in their ground states. Cr atoms induces magnetic moments on C atoms, building up an indirect exchange coupling through them. A measure of this coupling strength is the energy difference between AF and FM states. $\Delta E_{FM\rightarrow AF} = E_T(AF) - E_T(FM)$ is the energy required to flip the magnetic moment of one of the Cr atoms in the FM state and also its sign indicates the magnetic ground state favored by the $TM{-}C_n{-}TM$ chain. A comparision of our results with [10, 11, 31] is tabulated in Table 3.1. Except the case of

	Our Results		Previous Work	
n	ΔE(eV)	$\mu(\mu_B)$	ΔE(eV)	$\mu(\mu_B)$
0	-0.27	0(10)	N/A	N/A
1	1.22	8	1.12	8
2	-0.10	0(10)	-0.10	0(10)
3	1.06	8	0.87	8
4	-0.41	0(10)	-0.8	0(10)
5	0.89	8	0.70	8

Table 3.1: Comparison of our results with those in the literature [9,10] for isolated CrC_nCr chains. The energy difference of the AF and the FM states, $\Delta E_{FM\rightarrow AF} = E_T(AF){-}E_T(FM)$, and the magnetic moment μ of isolated CrC_nCr chains with $n = 0, 1, 2, 3, 4, 5$ is given. The sign of the energy difference indicates the magnetic ground state favoured by the structure,i.e. negative for AF and positive for FM cases. [For structures with AF ground states the moment corresponding to the FM excited states is also given in parenthesis.]

$n = 0$ in which Cr atoms interacts directly, the strength of the indirect exchange interaction decreases with increasing n(odd or even), as expected.

The magnetic moments of the atoms and the structure as a whole have been calculated by using Mulliken population analysis [39, 40] as it is implemented in ATK [41–43]. In agreement with previous studies[10, 11, 31] we observe that the distribution of atomic magnetic moments also depends on the number of C

atoms, n. It can be seen from Fig.3.2 that the relative alignment of the magnetic moments of Cr atoms are anti-parallel for CrC_nCr structures with even n and the situation is inverted for odd n (Fig.3.3). For both cases C atoms in between Cr atoms posses alternating magnetic moments.

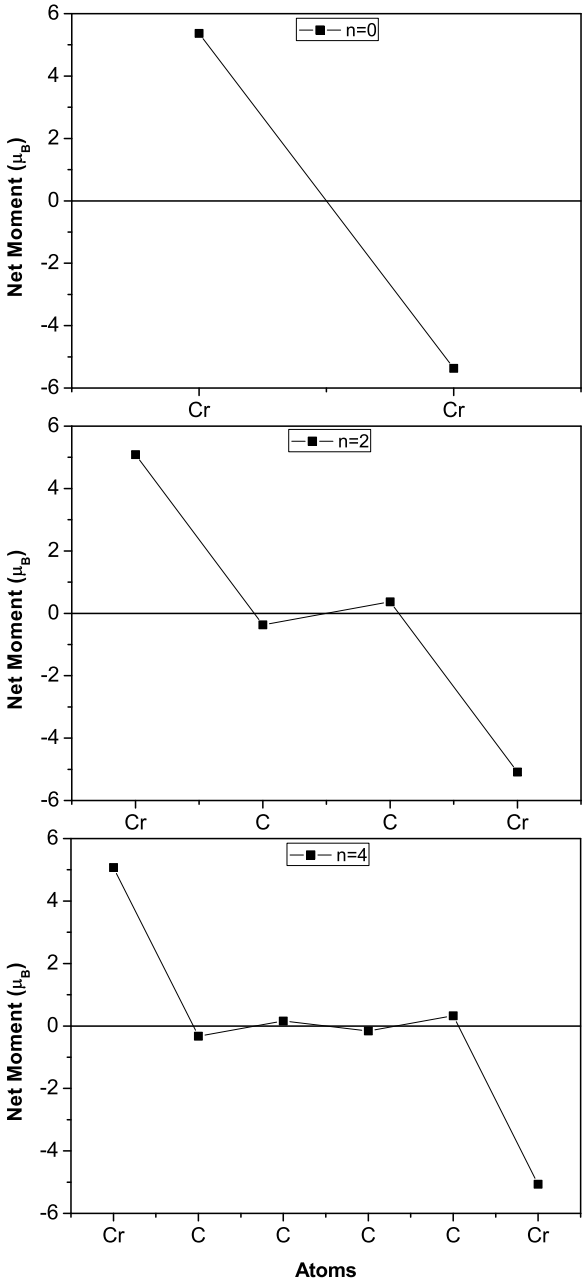

Figure 3.2: Variation of atomic magnetic moments of CrC_nCr for even n in their AF ground states

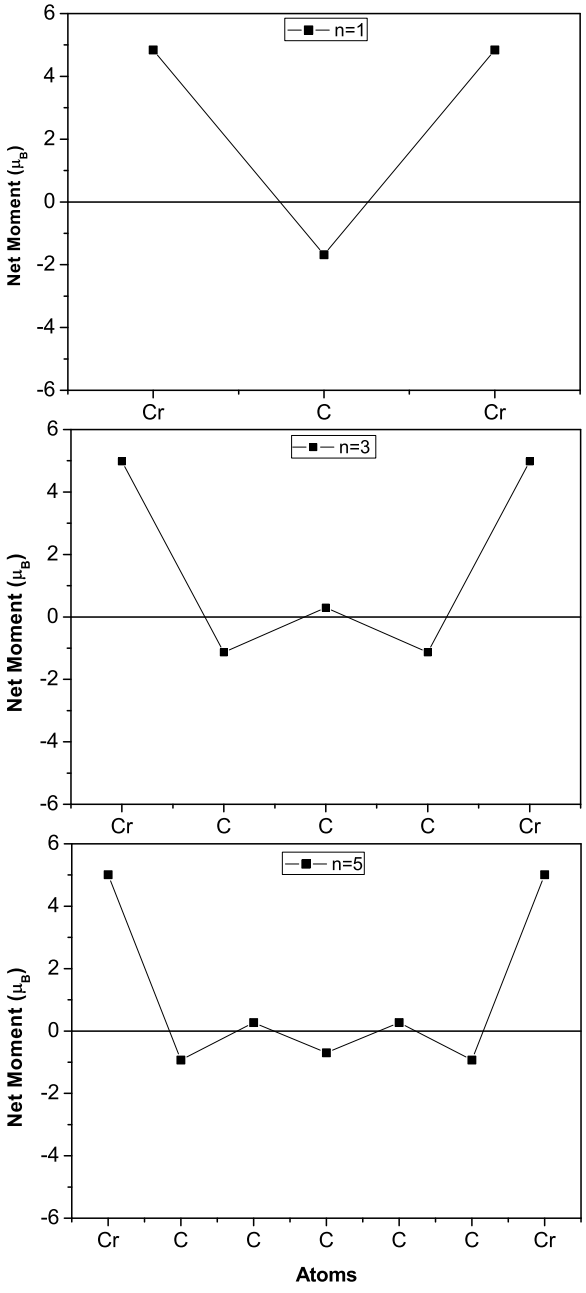

Figure 3.3: Variation of atomic magnetic moments of CrC_nCr for odd n in their FM ground states

These induced moments arise from spin-dependent states of Cr atoms. Their coupling distorts C states which are previously non-magnetic and creates spin-polarization through C atoms. Since this is an induced mechanism, the magnetic moment of the C atoms neighbouring to Cr atoms are greater than the inner ones. The decrease in interaction strength of Cr atoms with increasing n is also evident from the distribution of magnetic moments of C atoms. Much smaller moments are induced on C atoms, as Cr atoms are separated apart.

Not only electronic and magnetic properties of CrC_nCr is n dependent but also the molecular structure changes depending on n is being even or odd. If number of C atoms is odd, cumulene bonds are formed and the $C-C$ bond length does not vary significantly from its infinite counterpart of 1.30 Å. Polyyne bonds are formed for even n case and we observe large oscillations. The dimerization is evident in Fig.3.4 for CrC_nCr structures with odd n.

We have successfully obtained similar results with the literature for CrC_nCr chains. We have found that their structural, electronic and magnetic properties depends on n. This relation could be used as a tuning parameter to change the relative alignment of magnetization of Cr atoms and hence all of its electronic and transport properties. CrC_nCr structures are promising candidates for spintronics applications.

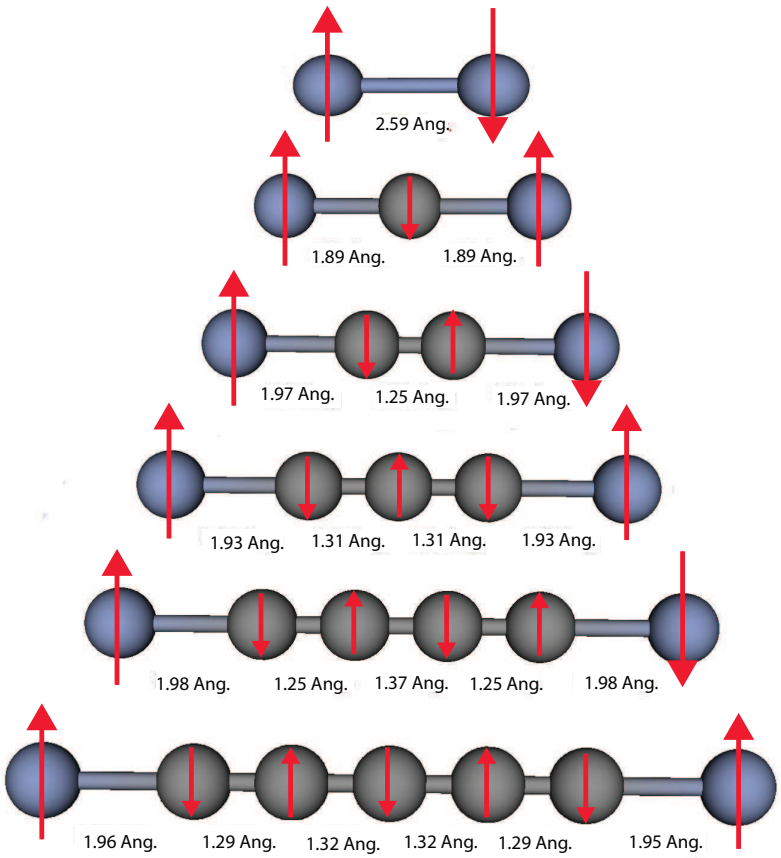

Figure 3.4: Optimized interatomic distances of CrC_nCr chains in their ground states

Chapter 4

Two-Probe Conductance Calculations of Transition Metal Caped Carbon Linear Chain

4.1 Two-Probe Geometry

In the conductance calculations the system is considered as composed of three parts: two electrodes and a scattering region positioned in between them as shown in Fig.4.1.

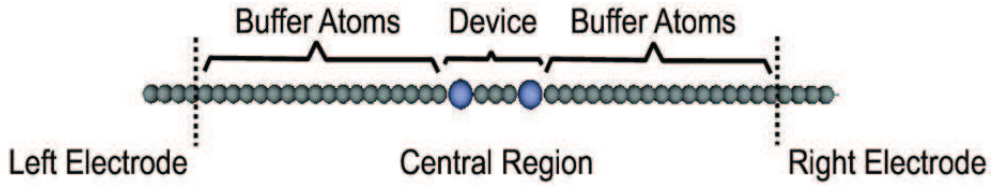

Figure 4.1: The geometric layout of the two-probe system that used in the conductance calculations: A TM-caped CLC positioned in-between the semi-infinite chains of carbon.

For the sake of simplicity semi-infinite carbon linear chains are chosen as electrodes. Although the active device is chromium caped carbon linear

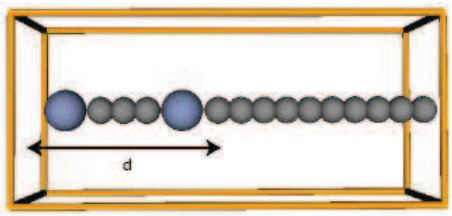

Figure 4.2: A view of the magnetic molecule connected to the electrodes: Light-blue corresponds to chromium atoms and grey corresponds to carbon.To find the space required for the molecule, atoms in the region d allowed to relax in position.

chain($CrCCr$), the surface atoms of the electrodes are included as buffer layers in the scattering region. Main role of these buffer layers is to screen the influence of the real scattering part (i.e., the molecule) such that the electrodes remains bulk-like.

Before building-up the two-probe geometry, the molecular bond-lengths of the device and its distance to the surface atoms of the electrodes are all together optimized within super cell geometry $a = 10$ Å, $b = 10$ Å, $c = L$ where L is the axial lattice parameter of the $CrC_nCr{-}C_{10}$ periodic structure as shown in Fig.4.2. The later 10 carbon atoms in the end stands for buffer layers that will be included in the scattering region in the two-probe calculations. To determine the electrode-electrode distance, d, we optimized the atomic coordinates of the molecule while the positions of the buffer atoms are held fixed. We have performed first-principles total energy calculations to obtain electronic structure and optimized geometry of $CrC_nCr{-}C_{10}$ periodic within density functional theory [19, 20] using the software package Atomistix ToolKit(ATK) [38] which combines non-equilibrium Green's function formalism to calculate the conductance properties in electrode-device-electrode geometry. The spin-dependent exchange-correlation potential is approximated within the generalized gradient approximation(GGA) [23]. Brillouin zone is sampled by 50 special k-point for the infinite CLC. The number of k-points is scaled according to size of the unit cell for $CrC_nCr{-}C_{10}$ periodic structures. For example, during the optimization calculations the

Brillouin zone is sampled by (1 1 3) k-points within the Monkhorst-Pack method [44]. Bloch wave functions have been expanded by double-zeta-polarized basis sets of local numerical orbitals whose kinetic energy is smaller than 200 Ryd. Atomic positions are optimized using steepest descent method. The convergence is achieved when the change in the total energy of the system between two successive ionic steps falls below 10^{-4} Ryd. and the Hellman-Feynman forces on the atoms falls below a tolerance of 0.01 eV/Å.

We observed that the magnetic ground state of the $CrC_nCr{-}C_{10}$ periodic structures strongly depends on n. In these periodic structures Cr atoms prefers to have anti-parallel magnetization(AF) for odd n and parallel magnetization(FM) for even n. As it is stated in the previous study, magnetic ordering in these structures is determined by the exchange interaction of transition metal atoms through non-magnetic carbon atoms [10, 11, 31]. The energy difference of the AF and the FM states, $\Delta E_{FM\rightarrow AF} = E_T(AF) - E_T(FM)$ for a $CrC_nCr{-}C_{10}$ periodic structure, indicates the coupling strength of the TM atoms., and it is tabulated in Table 4.1 for chromium, from $n = 0$ to 5. The sign of $\Delta E_{FM\rightarrow AF}$ shows the magnetic ground state of the structure, i.e. negative for AF and positive for FM cases. By comparing Tables 3.1 and 4.1, we learn that for molecular structures, the magnetic ground state is AF for even n and FM for odd n, whereas periodic structures shows an inverted behaviour. We conclude that CrC_nCr molecules changes magnetic ground state when connected to the electrodes. This opposition with the findings of [10, 11, 31] comes from difference in the choice of electrodes. Carbon electrodes couple better with carbon-based magnetic electrodes than gold electrodes, and as a result magnetic ground state of such structure changes when connected to the electrodes.

The magnetic moments of the atoms and the structure as a whole have been calculated by using Mulliken population analysis [39, 40] as it is implemented in ATK [41–43] and tabulated in Table 4.1. For those whose magnetic ground state is AF, the moment corresponding to the FM excited states is given in parenthesis. The non-integer magnetic moment values in the Table 4.1 could be a numerical artifact caused by interaction of Cr atoms in the neighbouring supercells because

n	d(Ang.)	ΔE(eV)	$\mu(\mu_B)$
0	6.84	0.88580	10
1	8.08	−0.39550	0(6)
2	9.33	1.48860	8
3	10.68	−0.38790	0(9.19)
4	11.98	0.44740	8
5	13.25	−0.34680	0(8.48)

Table 4.1: The electrode-electrode distance of the ground state, the energy difference of the AF and the FM states, $\Delta E_{FM\rightarrow AF} = E_T(AF) - E_T(FM)$, and the magnetic moment μ. The sign of the energy difference indicates the magnetic ground state favoured by the structure,i.e. negative for AF and positive for FM cases. [For structures with AF ground states the moment corresponding to the FM excited states is given in parenthesis.]

one-dimensional metallic structures are not very good at screening. Since the field strength of the external potential strongly depends on the length of the scattering region increased number of buffer layers up to 20 and 40 carbon atoms but the results are not improved. It is found that the magnetic ground state of $CrC_nCr - C_{10}$ periodic structures,is FM for even n while the structures with odd n prefer AF configuration as ground states. A typical example of this even-odd alternation is shown in Fig.4.3.

This optimized periodic structures are used while building-up the scattering region of the two-probe system that will be discussed in the next section.

4.2 Ground State Electronic and Magnetic Properties

Having determined the magnetic ground state and the distance, d, required for the molecule, we connect the rigid electrodes of carbon linear chains as shown in Fig.4.1. Here the choice of electrode is important since it determines overall conductance properties. Semi-infinite CLC are chosen as electrodes because it

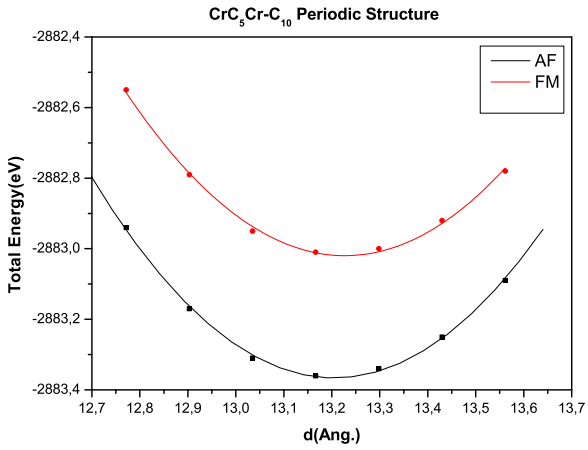

(a) n=odd

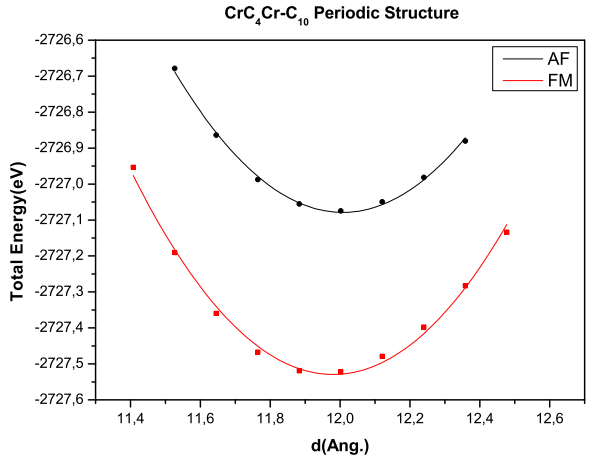

(b) n=even

Figure 4.3: Variation of the total energy of $CrC_nCr - C_{10}$ periodic structure as a function of distance, d. The equilibrium distance is determined by fitting a quadratic polynomial and taking its minimum, d_0. Atomic coordinates are also optimized for d_0. a)$d_0 = 11.98$ Åfor $n = 4$(up) and b)$d_0 = 13.25$ Åfor $n = 5$(down). Notice that the magnetic ground state is AF for $n = odd$ and FM for $n = even$.

is metallic and couples well with carbon-based structures. Of course in realistic systems this metallic property vanishes due to Peierls distortion [45]. This is why we used rigid electrodes and their corresponding buffer layers in the scattering region are also rigid, i.e without Peierls distortion.

After building-up the two-probe configuration, we first investigated the conductance properties of CrC_nCr molecules with $n = 0, 1, 2, 3, 4, 5$ at zero-bias. When there is no bias applied, chemical potentials of the electrodes, μ, are all aligned. The device is in equilibrium with the contacts. Even if the bias voltage is zero, one can mention finite conductance since it depends on the number of states available around $E = \mu$. Magnetic ground state of the CrC_nCr molecules connected to the electrodes are found to be AF for odd n and FM for even n. Thus, the molecular levels are spin-degenerate for odd n, and spin-splitted for even n. While spin-up and spin-down electrons contributes to the conductance equally for AF structures, the electrons(spin-up) whose spin alignment are the same with the alignment of the magnetic moments of the TM atoms contributes more in the FM structures.

Two examples of transmission and energy spectra with even and odd n is given in Fig.4.4 for zero-bias. Opposed to FM case, we do not observe any spin-polarization in the transmission spectrum of the AF system because molecular levels of an AF device are spin-degenerate. The reason why we observe smaller values in the transmission spectrum for the AF device can be explained in a similar fashion to the GMR effect. When the relative orientation of the magnetization of TM atoms changes from anti-parallel(AF) to parallel(FM), the material goes from a highly resistive state to a low resistance one. This is due to spin-dependent electron scattering. The resistance is high in the AF case because a spin-up electron at one end of CrC_nCr cannot go through to Cr(spin-down) at the other end due to suppressed spin-up density of states.

Moreover, the maximum of conduction is determined by the type of the electrodes. In the band structure of infinite CLC, the doubly degenerate π band crosses the Fermi level which accommodates two electrons per unitcell [46]. Thus, we expect to observe at most two for transmission coefficient around Fermi level.

The transmission spectrum of CrC_nCr two-probe system is enveloped by the transmission spectrum of infinite CLC.

Fig.4.4 shows also molecular levels of the CrC_nCr are affected when placed between between the two electrodes. These molecular levels are calculated by projecting the self-consistent Hamiltonian onto CrC_nCr atoms in the central region, and then diagonalized to produce an energy spectrum. Peaks in the transmission spectra can be interpreted as finger prints of molecular levels. We do not see a peak in the transmission spectrum for all of the levels in the energy spectrum because not all eigenstates of the projected Hamiltonian are open channels. Some of them localized in the scattering region, do not extend to the electrodes so do not contribute to the conduction. Furthermore, due to the coupling of the channel to the electrodes, the infinitely sharp molecular levels broaden and we observe broadened peaks in the transmission spectrum. At zero-bias we can only discuss the contribution of the levels close around $E = \mu$. However, under bias voltages levels higher and lower than μ begin to contribute to the conductance as we will discuss in the next section.

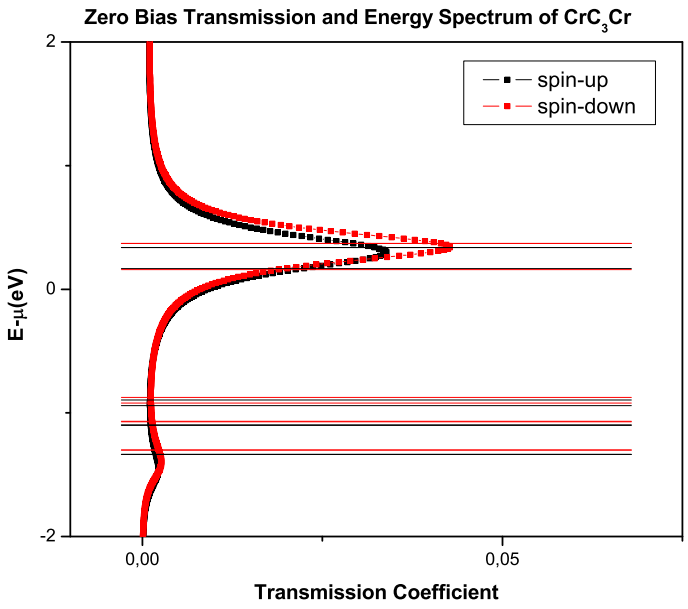

(a) n=odd

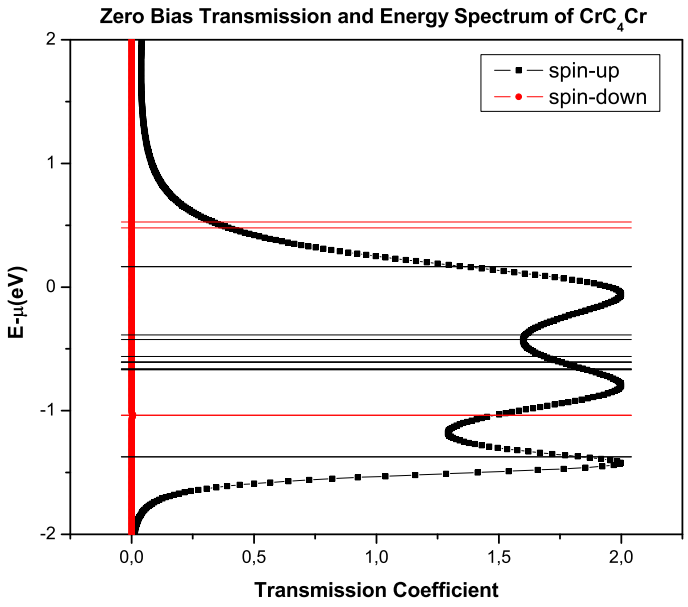

(b) n=even

Figure 4.4: The transmission and energy spectra of a)CrC_3Cr and b)CrC_4Cr two-probe systems at zero-bias. Average potential of the electrodes, μ, is set to zero.

4.3 Electronic and Magnetic Properties under Bias Voltages

Starting from the zero-bias calculation, we swept a range from -3.0V to 3.0V by slightly increasing(decreasing) the voltage in small steps of 0.05V for all $TM - C_n - TM$ structures with $n = 0, 1, 2, 3, 4, 5$. When we apply a bias voltage of V, actually the electrostatic potential of one of the electrode is risen by $\frac{eV}{2}$ and the other is lowered by $-\frac{eV}{2}$. Mainly the states around the average of the electrostatic potentials, i.e. the ones in the energy window from $\mu - \frac{eV}{2}$ to $\mu + \frac{eV}{2}$ contribute to the conduction. As we increase the voltage, the energy window of interest widens generally leading to inclusion of more channels. Sometimes due to re-alignment of the molecular levels at each bias, some levels slip out of the energy window.

The current-voltage characteristics and transport properties of CrC_nCr two-probe systems are found to be spin-polarized. Furthermore, polarization ratio changes with the applied voltage. The current-voltage characteristics of CrC_nCr structures strongly depends upon whether n is odd or even. The most remarkable property of the current curves is their family behaviour. All the curves of odd n follows the same trend (Fig.4.5), while those with even n follows a different one(Fig.4.6). These trends, however are in good agreement with our expectations from the zero-bias transmission spectra. As seen in from Fig.4.4, both spin-up and spin-down electrons contributes to the conduction for CrC_nCr structures with odd n, but there is contribution only from the spin-up electrons for structures with even n. This general trend is conserved in the current curves. Current transmitted from the structures with odd n is much smaller than that of the ones with even n. This difference can also be observed in the height of the peaks of zero-bias transmission spectra(Fig.4.4).

For a bias of V the potential of the left electrode is set to $\mu - \frac{V}{2}$ and the right electrode is set to $\mu + \frac{V}{2}$ in our calculations. So for positive bias values the current flows right to left and vice versa. Applying a reverse corresponds to negative current values for CrC_nCr two-probe systems with even n as shown in Fig.4.6. However, for CrC_nCr two-probe systems with odd n the situation is a

little different. Not only current changes sign but also I-V curves of spin-up and spin-down electrons interchange in Fig4.5. For such structures the magnetization of the Cr atoms are anti-parallel in their ground state. When the reverse current flows, electrons coming from the left electrode encounters Cr atom whose direction of the magnetization is opposite to the case of forward bias. and Fig.4.6. The I-V characteristics of the structures with the AF ground state display an interesting property. For forward bias the electrons coming from the right electrode first encounters with Cr atom whose direction of the magnetization is up. The electrons with same spin alignment scatter less. For reverse bias the situation is just the opposite.

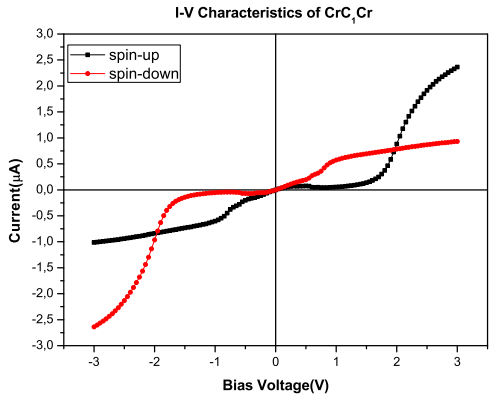

(a) n=1

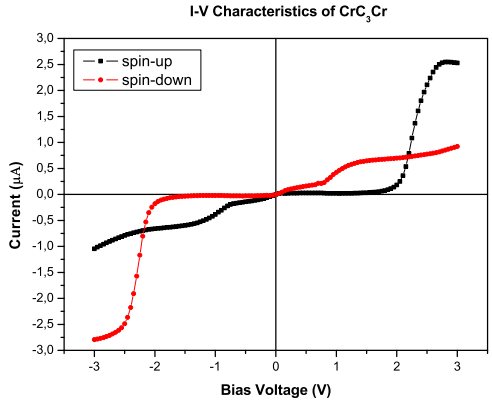

(b) n=3

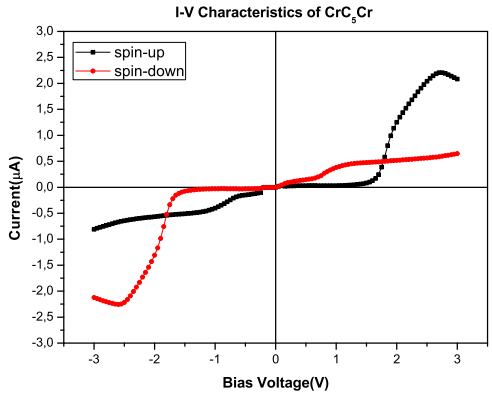

(c) n=5

Figure 4.5: Current-voltage characteristics for CrC_nCr two-probe systems with odd n.

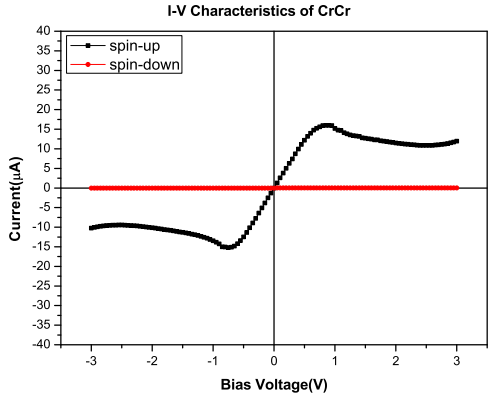

(a) n=0

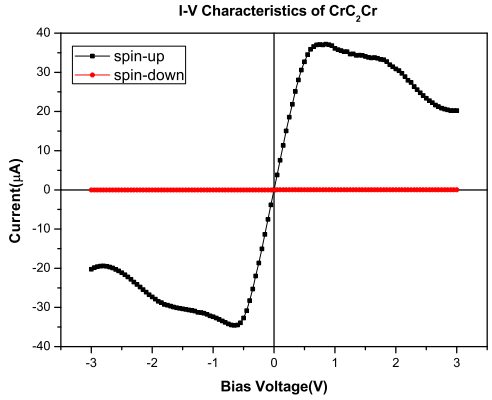

(b) n=2

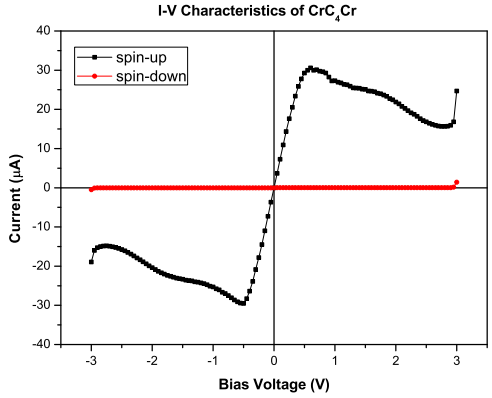

(c) n=4

Figure 4.6: Current-voltage characteristics for CrC_nCr two-probe systems with even n.

4.3.1 Two-probe Conductance Calculations of CrC_nCr with odd n

Although we do not optimize the structures under bias voltages, by investigating the change in the total energy of the two-probe system under bias, we concluded that the structure with odd n undergoes a magnetic transition. As we increase bias voltage, these initially AF materials attain net magnetic moments and FM configurations becomes ground states. Fig.4.7 shows the net magnetic moment induced in the scattering regions of initially AF CrC_3Cr two-probe system with $\mu = 0$ as we apply bias and its corresponding I-V curve is given in Fig.4.4a. From Fig.4.8 it is evident that the ground state undergoes a magnetic transition and changes to FM at 0.06V.

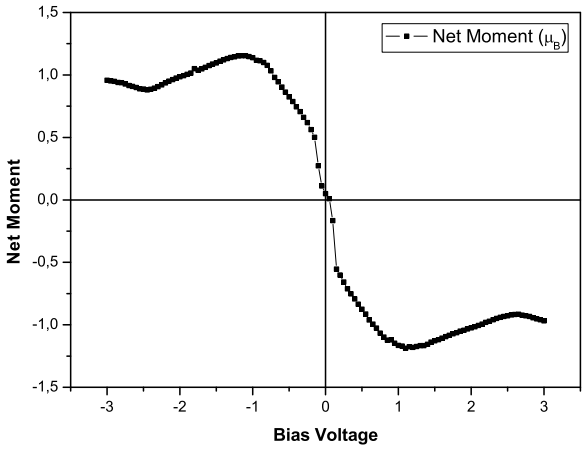

Figure 4.7: The net magnetic moment induced in the scattering regions of initially AF CrC_3Cr two-probe system with applied bias

At this critical voltage a net moment of $-0.08\mu_B$ is accumulated in the scattering region. While the magnetization of Cr atoms remain anti-parallel, the neighbouring C atoms get induced as seen from Fig.4.9.

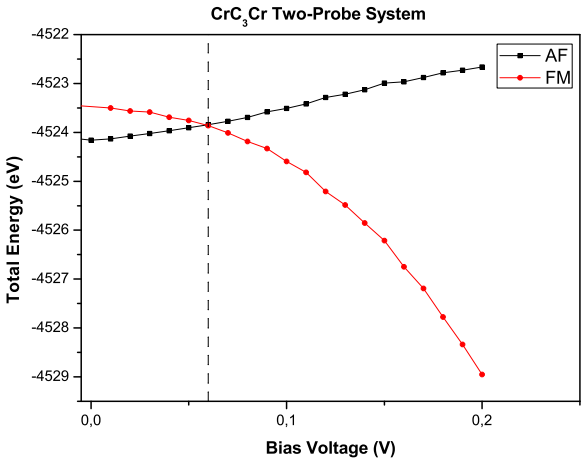

Figure 4.8: Change of magnetic ground state of CrC_3Cr two-probe system with applied bias

Then the current-voltage characteristics given in Fig.4.5 are no longer valid since they are calculated for two-probe system in which the alignment of the magnetic moments of Cr atom are anti-parallel(AF). However, the material remains in that state up to a critical voltage(0.06V for CrC_3Cr two-probe system). After that critical voltage current should be calculated for CrC_nCr two-probe systems with odd n in which the alignment of the magnetic moments of Cr atom are parallel(FM). For example, the current-voltage characteristics of CrC_3Cr two-probe system for forward bias is given in Fig.4.10. The FM characteristics is dominant in the I-V curve, after the transition the current transmitted is 100% spin-polarized. For very small biases when the AF configuration is valid, both spin-up and spin-down electrons contribute to the conduction equally due to non-degenerate molecular levels and then levels begin to split resulting in split in the I-V curves. After the transition(FM domain) the current increases linearly with bias, but after a while the slope of the curve changes. After 2.5V current transmitted decreases with applied bias and we observe negative differential resistance(NDR).

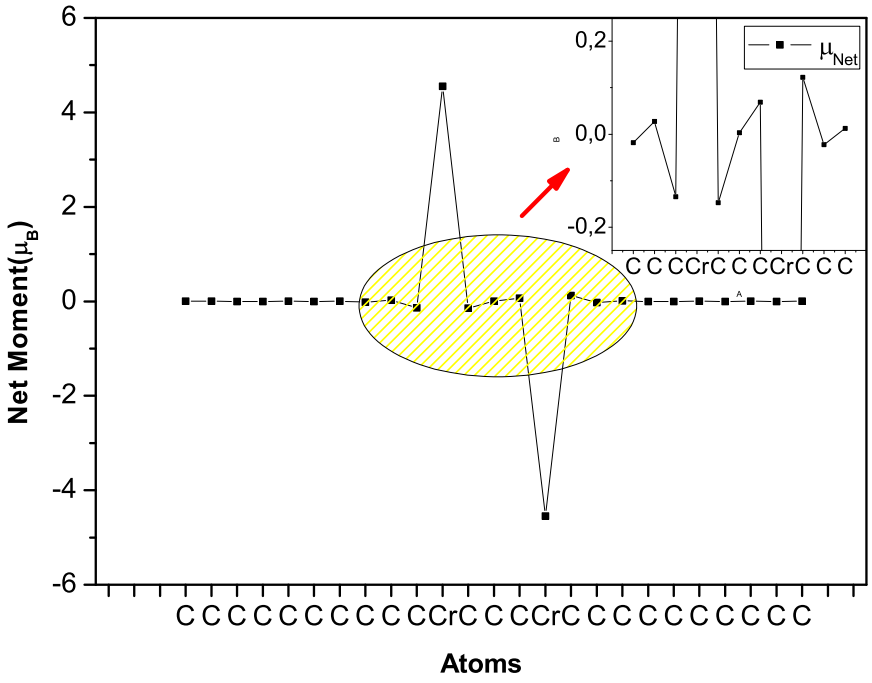

Figure 4.9: Variation of atomic magnetic moments in the scattering region of CrC_3Cr two-probe system at 0.06V

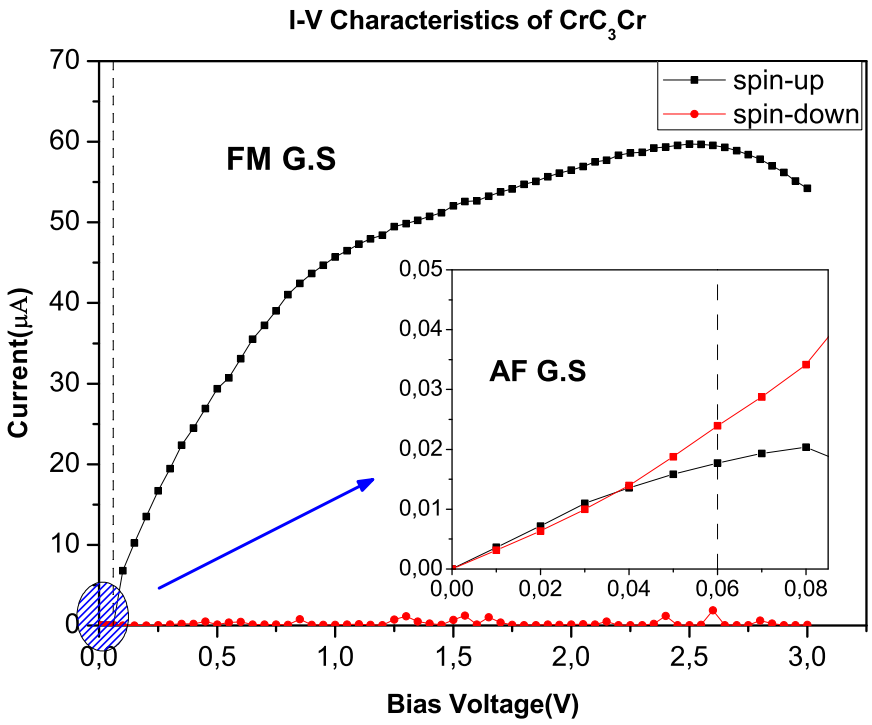

Figure 4.10: The current-voltage characteristics CrC_3Cr two-probe system for forward bias. The inset shows when the AF configuration is valid.

The trends in the current-voltage characteristics can be explained by inspecting transmission and energy spectra under bias. Since for FM system there is no contribution from spin-down electrons, we carry out the discussion based on spin-down spectra. The current is related to the integral of the transmission function in the energy window of interest. For small biases the current transmitted is also small because the the range of integration is narrow. As it can seen from Fig.4.11, despite absence of a molecular level in the window, we have finite current at 0.5V just because the tail of a broadened level centred around 3.0eV enters the window. As we go through 1.0V, the current increases because the window widens including a level(and a corresponding peak). So the area under the curve becomes larger. After 1.0V the current increases with bias displaying slower trend because there is no new level to enter the window. Moreover, the transmission and the energy spectra of the system at 1.5V given in Fig.4.11 tell us that, the molecular levels align themselves with bias. The peak of the transmission function slipped down with the molecular levels. Even if the integration range is large, the current does not increase in the same fashion since the area under the transmission function is small.

Two mechanisms play role in NDR. The first one is the escape of molecular levels from the energy window of interest. This is due to re-alignment of the levels with the contact potential. The other one is narrowing of the peaks of the transmission spectrum. In Fig.4.12, as the bias increases there is no new level to enter the energy window. Besides the levels slip down. They do not escape from the window, but the corresponding transmission peaks also slip down and get narrower. The area under the curve reduces and as a result the current decays.

Since the polarization ratio is 100% except for very small biasses, CrC_nCr with odd n behaves as perfect spin-filters and can be utilized for spintronic applications.

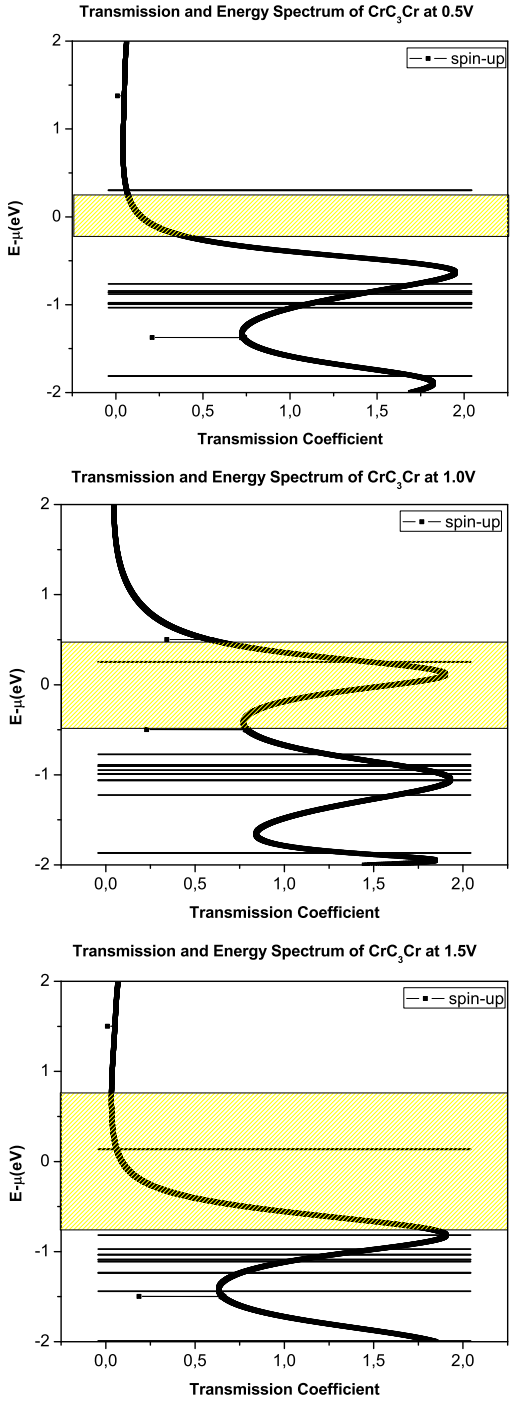

Figure 4.11: The transmission and energy spectra of CrC_3Cr two-probe systems at 0.5V, 1V and 1.5V. Energy window of interest shaded with yellow. Average potential of the electrodes, μ, is set to zero.

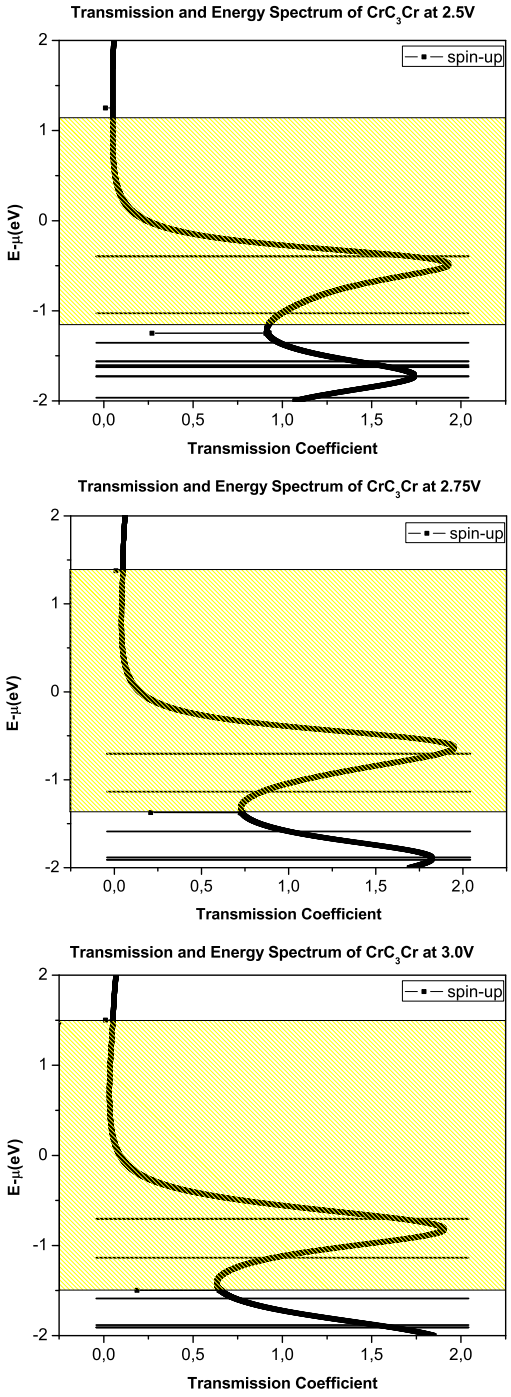

Figure 4.12: The transmission and energy spectra of CrC_3Cr two-probe systems at 2.5V, 2.75V and 3.0V. Energy window of interest shaded with yellow. Average potential of the electrodes, μ, is set to zero.

4.3.2 Two-probe Conductance Calculations of CrC_nCr with even n

As mentioned earlier in Section 4.1, when there are an even number carbon atoms in between chromium atoms, the orientation of the magnetic moments of chromium atoms becomes parallel. When they are parallel, the magnetic ground state of the material is FM and the molecular energy levels become spin-dependent as shown in Fig.4.4a. This spin dependency of molecular energy levels manifests itself in the transmission spectrum and as a result the current, which is nothing but integration of the transmission function in the energy window of interest, becomes spin-polarized. A characteristic example of current-voltage curve of such structures for forward bias is shown in Fig.4.14a. Two-probe conductance properties of the AF excited state of the same structure is also calculated and no change in the ground state is observed(Fig.4.13).

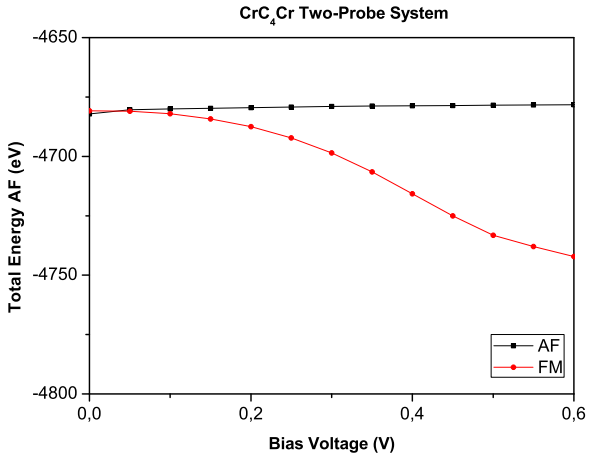

Figure 4.13: Variation total energy of CrC_4Cr two-probe system FM ground state and AF excited state

For small biases, the current increases with the voltage applied but after a while it gets saturated and we also observe NDR at high bias values. The

current transmitted is fully spin-polarized(Fig.4.14b). The general trend of I-V curve is very similar to FM domain of CrC_nCr two-probe systems with odd n. The same discussions apply, and we do not repeat them here. The sudden change in the current value at $3.0V$ is due to inclusion of a spin-down conducting channel at 1.5eV. As seen from Fig.4.15b at $3.0V$ the energy window lies from -1.5eV to 1.5eV and at the boundary there is a sharp peak coming from a newly included spin-down channel. The narrow width of the corresponding peak in the transmission spectrum suggests that the level is not broadened due to coupling with the contacts.

We observed spin-valve behaviour in CrC_nCr magnetic molecules and the spin-polarization ratio can be tuned by applied voltage. CrC_nCr chains are the molecular analogue of conventional GMR devices.

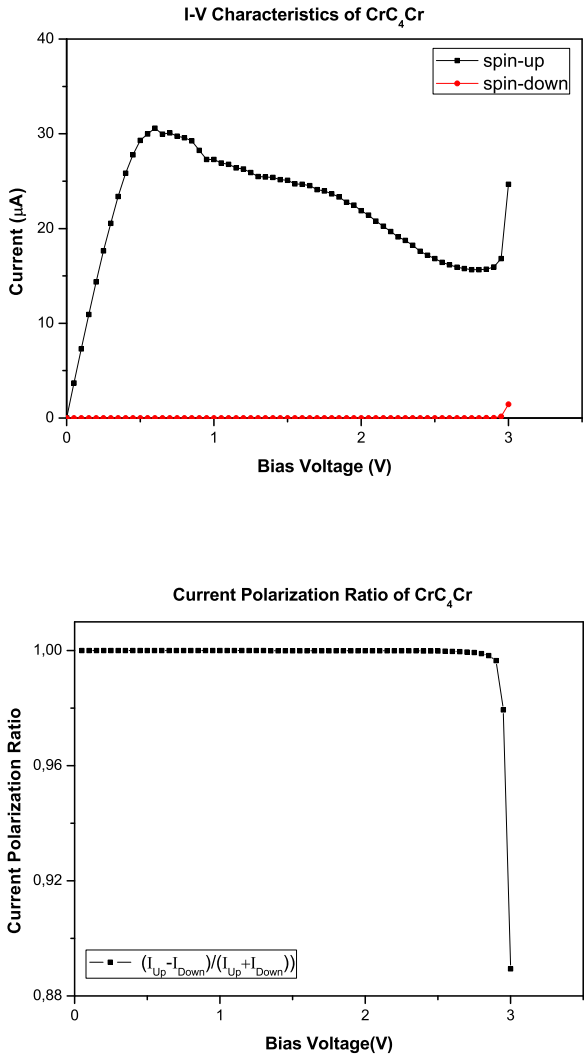

Figure 4.14: a)The current-voltage characteristics and b)the spin-polarization ratio of the transmitted current from CrC_4Cr molecule for forward bias

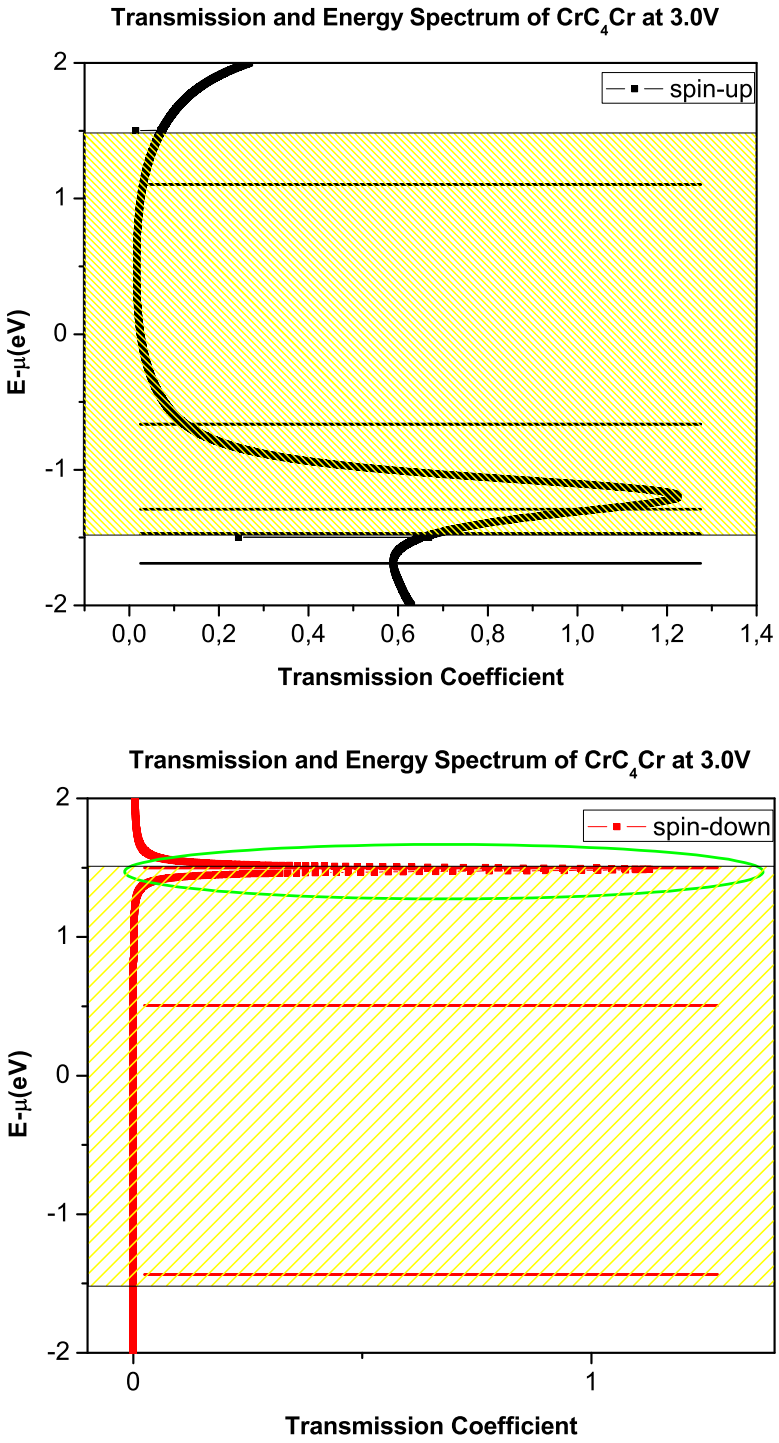

Figure 4.15: The transmission and energy spectra of CrC_4Cr two-probe systems at 3.0V. Energy window of interest shaded with yellow. Average potential of the electrodes, μ, is set to zero.

Chapter 5

Conclusions

In this study, we inspected CrC_nCr atomic chains for creating spin-polarized currents. The obtained results are briefly summarized below.

At the beginning the spin dependent structural, electronic and magnetic properties of CrC_nCr molecules studied earlier by Durgun et al. are reproduced out using first-principle methods. In agreement with earlier studies we have found that the structural, electronic and magnetic properties of CrC_nCr molecular structures strongly depends on the number of C atoms in between the Cr atoms, n. The magnetic Cr atoms interacts indirectly through C atoms inducing alternating net magnetic moments on them. The strength of this indirect exchange interaction decreases with increasing n and smaller moments are induced on C atoms. The ground state magnetic configuration and the net magnetic moment attained by these structures are also determined by n. The relative magnetization of Cr atoms are parallel(FM) for odd n, whereas it is anti-parallel for even n. FM structures posses a net moment of $8\mu_B$. The $C{-}C$ bonds in these chains are cumulene like for odd n and polyyne like for even n. The n dependency of the magnetic ground state can be used as a tuning parameter to change the relative alignment of magnetization of Cr atoms and hence all of its electronic and transport properties. CrC_nCr structures are promising candidates for spintronic applications.

Periodic atomic chains of $CrC_nCr{-}C_{10}$ are also studied to investigate the

effect of the electrodes. Opposing to the previous works which used Au electrodes, we found that the magnetic ground state of atomic chains change when they are coupled with semi-infinite CLC electrodes. This difference in the results comes from the choice of the electrodes.

Gaining information about CrC_nCr atomic chains, we calculated their two-probe conductance properties under zero and finite biases using rigid semi-infinite CLC electrodes. The current-voltage characteristics of CrC_nCr structures strongly depends upon whether n is odd or even. For AF structure with odd n, the current transmitted is relatively small due spin-dependent scattering of electrons from both contacts. However, further investigation of such systems showed that the ground state changes to FM after a critical bias-voltage and then FM characteristics is mostly dominant I-V curves. We do not see such transition for FM systems. The trends in the current voltage characteristics are explained by comparing corresponding transmission spectra and molecular energy levels under bias. Negative differential resistance is observed for both structures with even and odd n at high biases. This is due to slip of molecular levels from energy window of interest and narrowing of the peaks of the transmission spectrum.

Our result here suggests that to control the spin-polarization of the current transmitted from CrC_nCr spin-valves, there is no need to apply external magnetic fields because the switching occurs due to applied bias. The natural ground state of CrC_nCr two-probe systems with odd n has an anti-parallel(AF) spin configuration and their magnetic ground state changes to FM with applied voltage. Thus, we have a spin-valve which is initially in 'off-state' turned on with applied bias. On the other hand the magnetic ground state of CrC_nCr two-probe systems with even n is FM and remains in that state under bias. The current transmitted through them is 100% spin-polarized for both low and high bias values. Thus they behave as perfect spin-filters.

Bibliography

[1] M. Baibich, J. Broto, A. Fert, F. Van Dau, F. Petroff, P. Etienne, G. Creuzet, A. Friederich, and J. Chazelas, "Giant magnetoresistance of (001) Fe (001) Cr magnetic superlattices," *Physical Review Letters* **61**, no. 21, 2472–2475 (1988).

[2] G. Binasch, P. Gr
"unberg, F. Saurenbach, and W. Zinn, "Enhanced magnetoresistance in layered magnetic structures with antiferromagnetic interlayer exchange," *Physical Review B* **39**, no. 7, 4828–4830 (1989).

[3] S. Sanvito and A. Rocha, "Molecular-Spintronics: the art of driving spin through molecules," *Arxiv preprint cond-mat/0605239* (2006).

[4] S. Wolf, D. Awschalom, R. Buhrman, J. Daughton, S. Von Molnar, M. Roukes, A. Chtchelkanova, and D. Treger, "Spintronics: A spin based electronics vision for the future," *Science* **294**, no. 5546, 1488–1495 (2001).

[5] L. Bogani and W. Wernsdorfer, "Molecular spintronics using single-molecule magnets," *Nature Materials* **7**, no. 3, 179–186 (2008).

[6] A. Pasupathy, R. Bialczak, J. Martinek, J. Grose, L. Donev, P. McEuen, and D. Ralph, "The Kondo effect in the presence of ferromagnetism," *Science* **306**, no. 5693, 86–89 (2004).

[7] L. Hueso, J. Pruneda, V. Ferrari, G. Burnell, J. Valdés-Herrera, B. Simons, P. Littlewood, E. Artacho, A. Fert, and N. Mathur, "Transformation of

spin information into large electrical signals using carbon nanotubes," *Nature* **445**, no. 7126, 410–413 (2007).

[8] R. De Groot, F. Mueller, P. Engen, and K. Buschow, "New class of materials: Half-metallic ferromagnets," *Physical Review Letters* **50**, no. 25, 2024–2027 (1983).

[9] S. Dag, S. Tongay, T. Yildirim, E. Durgun, R. Senger, C. Fong, and S. Ciraci, "Half-metallic properties of atomic chains of carbon–transition-metal compounds," *Physical Review B* **72**, no. 15, 155444 (2005).

[10] E. Durgun, R. Senger, H. Mehrez, H. Sevinçli, and S. Ciraci, "Size-dependent alternation of magnetoresistive properties in atomic chains," *The Journal of chemical physics* **125**, 121102 (2006).

[11] E. Durgun, R. Senger, H. Sevinçli, H. Mehrez, and S. Ciraci, "Spintronic properties of carbon-based one-dimensional molecular structures," *Physical Review B* **74**, no. 23, 235413 (2006).

[12] M. Born and J. R. Oppenheimer, "Zur Quantentheorie der Molekeln," *Annalen der Physik* **84**, 457 (1927).

[13] D. Hartree, "Cambridge Philos," *Soc* **24**, 89 (1928).

[14] V. Fock, "Naherungsmethode zur Losung des quantenmechanischen Mehrkorperproblems," *Zeitschrift fur Physik A Hadrons and Nuclei* **61**, no. 1, 126–148 (1930).

[15] V. Fock and Z. Physik, "61, 126 (1930) JC Slater," *Phys. Rev* **35**, 210 (1930).

[16] L. H. Thomas *Proc. Cambridge Phil. Roy. Soc.* **23**, 542 (1927).

[17] E. Fermi *Rend. Accad. Naz. Lincei.* **6**, 602 (1927).

[18] P. A. M. Dirac *Proc. Cambridge Phil. Roy. Soc.* **26**, 376 (1930).

[19] P. Hohenberg and W. Kohn, "Inhomogeneous electron gas," *Phys. Rev* **136**, no. 3B, B864–B871 (1964).

[20] W. Kohn, L. Sham, *et al.*, "Self consistent equations including exchange and correlation effects," *Phys. Rev* **140**, no. 4A, A1133–A1138 (1965).

[21] R. Stowasser and R. Hoffmann *Journal of the Americal Chemical Society* **121**, 3414 (1999).

[22] D. Ceperley and B. Alder, "Ground state of the electron gas by a stochastic method," *Physical Review Letters* **45**, no. 7, 566–569 (1980).

[23] J. Perdew, K. Burke, and M. Ernzerhof, "Generalized gradient approximation made simple," *Physical Review Letters* **77**, no. 18, 3865–3868 (1996).

[24] M. Frisch, G. Trucks, H. Schlegel, P. Gill, B. Johnson, M. Robb, J. Cheeseman, T. Keith, G. Petersson, J. Montgomery, *et al.*, "Gaussian 94, Revision B. 2, Gaussian, Inc., Pittsburgh, PA, 1995. Ž. 17. AD Becke," *Phys. Rev. A* **38**, 3098 (1988).

[25] J. P. Perdew and Y. Wang, "Accurate and simple analytic representation of the electron-gas correlation energy," *Phys. Rev. B* **45**, 13244–13249(Jun, 1992).

[26] R. Landauer, "Electrical resistance of disordered one dimensional lattices," *Philosophical magazine* **21**, no. 172, 863–867 (1970).

[27] S. Datta, *Quantum transport atom to transistor*. Cambridge Univ Pr, 2005.

[28] R. Pati, M. Mailman, L. Senapati, P. Ajayan, S. Mahanti, and S. Nayak, "Oscillatory spin-polarized conductance in carbon atom wires," *Physical Review B* **68**, no. 1, 14412 (2003).

[29] R. Pati, L. Senapati, P. Ajayan, and S. Nayak, "First-principles calculations of spin-polarized electron transport in a molecular wire: Molecular spin valve," *Physical Review B* **68**, no. 10, 100407 (2003).

[30] L. Senapati, R. Pati, M. Mailman, and S. Nayak, "First-principles investigation of spin-polarized conductance in atomic carbon wires," *Physical Review B* **72**, no. 6, 64416 (2005).

[31] E. Durgun, *Spintronic properties of carbon and silicon based nanostructures*. PhD thesis, Ph. D. Dissertation. Bilkent: Bilkent University, 2007.

[32] S. Tongay, R. Senger, S. Dag, and S. Ciraci, "Ab-initio electron transport calculations of carbon based string structures," *Physical review letters* **93**, no. 13, 136404 (2004).

[33] G. Roth and H. Fischer, "On the Way to Heptahexaenylidene Complexes: Trapping of an Intermediate with the Novel MCCCCCCCR2 Moiety," *Organometallics* **15**, no. 26, 5766–5768 (1996).

[34] Y. Liu, R. Jones, X. Zhao, and Y. Ando, "Carbon species confined inside carbon nanotubes: A density functional study," *Physical Review B* **68**, no. 12, 125413 (2003).

[35] E. Cazzanelli, L. Caputi, M. Castriota, A. Cupolillo, C. Giallombardo, and L. Papagno, "Carbon linear chains inside multiwalled nanotubes," *Surface Science* **601**, no. 18, 3926–3932 (2007).

[36] V. Scuderi, S. Scalese, S. Bagiante, G. Compagnini, L. D′Urso, and V. Privitera, "Direct observation of the formation of linear C chain/carbon nanotube hybrid systems," *Carbon* (2009).

[37] C. Jin, H. Lan, L. Peng, K. Suenaga, and S. Iijima, "Deriving Carbon Atomic Chains from Graphene," *Physical Review Letters* **102**, no. 20, 205501 (2009).

[38] Q. A/S, "Atomistix toolkit version 2008.10.0,,".

[39] R. Mulliken, "Electronic Population Analysis on LCAO [Single Bond] MO Molecular Wave Functions. II. Overlap Populations, Bond Orders, and

Covalent Bond Energies," *The Journal of Chemical Physics* **23**, 1841 (1955).

[40] I. Csizmadia, *Theory and Practice of MO calculations on Organic Molecules*. Elsevier Science & Technology, 1976.

[41] M. Brandbyge, J. Mozos, P. Ordejon, J. Taylor, and K. Stokbro, "Density-functional method for nonequilibrium electron transport," *Physical Review B* **65**, no. 16, 165401 (2002).

[42] J. Soler, E. Artacho, J. Gale, A. Garcia, J. Junquera, P. Ordejon, and D. Sánchez-Portal, "The SIESTA method for ab initio order-N materials simulation," *Journal of Physics Condensed Matter* **14**, no. 11, 2745–2780 (2002).

[43] J. Taylor, H. Guo, and J. Wang, "Ab initio modeling of quantum transport properties of molecular electronic devices," *Physical Review B* **63**, no. 24, 245407 (2001).

[44] H. J. Monkhorst and J. D. Pack, "Special points for brillouin-zone integrations,"*Phys. Rev. B* **13**, 5188–5192(Jun, 1976).

[45] R. Peierls, *Quantum theory of solids*. Oxford University Press, USA, 2001.

[46] S. Tongay, S. Dag, E. Durgun, R. Senger, and S. Ciraci, "Atomic and electronic structure of carbon strings," *Journal of Physics, Condensed Matter* **17**, no. 25, 3823–3836 (2005).